



Coeloglossum viride var. *bracteatum* attenuates lipopolysaccharide-induced acute depressive-like behaviors in mice by inhibiting neuroinflammation and protecting synaptic plasticity

Zhe Guo^{a,1}, Jinpeng Bai^{b,1}, Jun Wang^b, Xiuyuan Lang^d, Min-Min Cao^b, Si-Jia Zhong^e, Liang Cui^a, Yang Hu^b, Xiao-Yan Qin^{b,*}, Rongfeng Lan^{c,*}

^a The Emergency Department, The Third Affiliated Hospital of Guangxi Medical University, Nanning 530021, China

^b Key Laboratory of Ecology and Environment in Minority Areas National Ethnic Affairs Commission, Center on Translational Neuroscience, College of Life and Environmental Sciences, Minzu University of China, Beijing 100081, China

^c Department of Cell Biology & Medical Genetics, College of Basic Medical Sciences, Shenzhen University School of Medicine, Shenzhen 518060, China

^d Department of Genetics and Genome Sciences, School of Medicine, Case Western Reserve University, Cleveland, OH 44106, USA

^e Khoury College of Computer Science, Northeastern University Seattle Campus, Seattle, WA 98109, USA

ARTICLE INFO

Keywords:

HIF-1 α
PKM2
LPS
HPA axis
OXPHOS
Synaptic plasticity

ABSTRACT

Microglia-mediated neuroinflammation and synaptic damage contribute to the pathogenesis of major depressive disorder. *Coeloglossum viride* var. *bracteatum* extract (CE) has anti-inflammatory and neuroprotective effects. Therefore, we hypothesized that CE could inhibit the pathogenesis of depression. To test this hypothesis, we evaluated the antidepressant effects of CE in a lipopolysaccharide (LPS)-induced mouse model. We showed that CE ameliorated LPS-induced depressive-like phenotypes such as increased preference for sucrose, decreased immobility, and improved willingness to move in mice. Consistently, CE reduced the levels of pro-inflammatory cytokines TNF- α , IL-1 β , and IL-6 in the brain. Mechanistically, CE transformed the phenotypic polarization of microglia by inhibiting the enhancement of aerobic glycolysis and improving oxidative phosphorylation, mediated by the HIF-1 α /PKM2 signaling axis. CE reversed the reduction in synaptic proteins, dendritic spines, and neuronal loss. Thus, CE may alleviate LPS-induced depression through anti-inflammation, alteration of microglial energy metabolism and protection of synaptic plasticity, thus highlighting its potential as antidepressant.

1. Introduction

Major depressive disorder (MDD) is a prevalent mental health problem that severely burdens society due to its high risk of morbidity and increased risk of suicide. It is projected to be the leading cause of mental health-related disability worldwide (Malhi & Mann, 2018; Marwaha et al., 2023). The prevalence of depression is increasing every year, with 300 million people (about 3.75 %) suffering from MDD globally, it has become one of the leading causes of disability.

Depression is projected to be the number one disease burden by 2030 (Cui et al., 2024; Marx et al., 2023). Current clinical pharmacotherapy for the treatment of MDD emphasize the efficacy of antidepressants based on the monoamine hypothesis (Krishnan & Nestler, 2008), while psychological interventions, social support, and exercise are also considered essential adjunctive therapies (Marwaha et al., 2023). However, between one-third and two-thirds of MDD patients are still ineffective on multiple antidepressant therapies and may experience adverse effects. The underlying pathogenesis of MDD goes far beyond

Abbreviations: CE, *Coeloglossum viride* var. *bracteatum* extract; MDD, major depressive disorder; TNF- α , tumor necrosis factor alpha; IL-6, interleukin-6; IL-1 β , interleukin-1 β ; LPS, lipopolysaccharide; CNS, central nervous system; IL-10, interleukin-10; OXPHOS, oxidative phosphorylation; PFC, prefrontal cortex; HIP, hippocampus; OFT, open field test; TST, tail suspension test; FST, forced swimming test; SPT, sucrose preference test; ALT, alanine aminotransferase; GOT, glutamic oxaloacetic transaminase; SOD, superoxide dismutase; CAT, catalase; MDA, malondialdehyde; ELISA, enzyme-linked immunosorbent assay; HK, hexokinase; PK, pyruvate kinase; PDH, pyruvate dehydrogenase; ANOVA, analysis of variance; DG, dentate gyrus; SYP, synaptophysin; HPA, hypothalamic-pituitary-adrenal.

* Corresponding authors.

E-mail addresses: bjqinxiaoyan@muc.edu.cn (X.-Y. Qin), lan@szu.edu.cn (R. Lan).

¹ These authors contribute equally: Zhe Guo and Jinpeng Bai.

<https://doi.org/10.1016/j.jff.2024.106526>

Received 21 April 2024; Received in revised form 8 July 2024; Accepted 13 October 2024

Available online 22 October 2024

1756-4646/© 2024 The Authors. Published by Elsevier Ltd. This is an open access article under the CC BY-NC license (<http://creativecommons.org/licenses/by-nc/4.0/>).

simple monoamine mechanism (Li, Ruan, Chen, & Fang, 2021). Growing evidence supporting an association between MDD and neuroinflammation has raised interest in use of immune system as therapeutic approach to MDD. There is evidence that proinflammatory cytokines such as tumor necrosis factor alpha (TNF- α), interleukin-6 (IL-6) and interleukin-1 β (IL-1 β) are at elevated levels in individuals with MDD. Targeting these proinflammatory cytokines has antidepressant potential (Miller, Maletic, & Raison, 2009; Miller & Raison, 2016). For instance, neuroinflammation induced by various sources such as bacterial endotoxin lipopolysaccharide (LPS) can be reversed by anti-inflammatory drugs such as ibrutinib (Li, Ali, et al., 2021), and herbal medicines, including bergapten (Yan et al., 2023), which in turn alleviate depressive-like behaviors.

Microglia are the main resident immune cells in the central nervous system (CNS) and play a critical role depending on their activation status. Initial activation of microglia has anti-inflammatory effects, whereas chronic activation has been implicated in the pathogenesis of various neurological disorders through the promotion of neuroinflammation (Woodburn, Bollinger, & Wohleb, 2021). Elevated microglia activation has been observed in the ventral prefrontal lobe of suicidal individuals (Schneider et al., 2014). Notably, activated microglia release pro-inflammatory cytokines that trigger hypothalamic–pituitary–adrenal (HPA) axis activation and peripheral glucocorticoid secretion during MDD (Enache, Pariante, & Mondelli, 2019; Felger & Lotrich, 2013). In turn, glucocorticoids regulate microglia activation and the HPA axis (Walker & Spencer, 2018). In addition, an imbalance between the two microglia phenotypes (M1 and M2) has been reported to contribute to the pathophysiology of depression (Burke, Kerr, Moriarty, Finn, & Roche, 2014; Zhang, Zhang, & You, 2018). The M1-type exerts pro-inflammatory effects, releasing cytokines such as TNF- α , IL-6 and IL-1 β , which mediate inflammation and influence the pathogenesis of depression (Zhang et al., 2018). Conversely, the M2 phenotype promotes anti-inflammatory responses. Targeting the modulation of microglial phenotype polarization has become the focus of antidepressant development. For example, chronic administration of minocycline in animal models of depression not only suppresses the activation of M1-type microglia and reduces IL-1 β expression, but also enhances the activity of M2 phenotype microglia and increases the expression of the anti-inflammatory cytokine IL-10. This underscores the pivotal role of microglial polarization in modulating the depressive phenotype (Burke et al., 2014). Therefore, the switch of microglia from M1 phenotype to M2 phenotype may be a potentially effective strategy for treating MDD (Guo, Wang, & Yin, 2022; Zhang et al., 2018). Furthermore, recent studies have revealed the metabolic mechanisms underlying the phenotypic switch in microglia, in particular the transition from aerobic glycolysis to oxidative phosphorylation (OXPHOS) (Orihuela, McPherson, & Harry, 2016). When exposed to inflammatory stimuli such as LPS, M1-type microglia have increased lactate production, ATP consumption, and reliance on aerobic glycolysis. However, with anti-inflammatory treatment, energy metabolism of microglia tends to favor OXPHOS (Ghosh, Castillo, Frias, & Swanson, 2018; Nair et al., 2019). Recent studies also have reported regulation of microglial energy metabolism is promising for neurological disorder (Pan et al., 2022), as well as for MDD (Peng et al., 2021; Sakrajda & Szczepankiewicz, 2021).

Converging evidence demonstrates that synaptic plasticity is central to the pathogenesis of MDD. From clinical reports to animal models, branch-specific elimination of dendritic spines and neuronal loss in key brain regions, such as hippocampus (HIP) and prefrontal cortex (PFC), have been associated with depressive states (Cao et al., 2021; Kim, Rapoport, & Rao, 2010; Moda-Sava et al., 2019; Parekh, Johnson, & Liston, 2022). In addition, the expression of a variety of genes involved in synaptic function is reduced in patients with multiple depressive disorders, whereas antidepressants increase the expression levels of these genes (Price & Drevets, 2010). For example, the *d*-stereoisomer of methadone exerts a rapid antidepressant effect through regulating

mTORC1-mediated synaptic plasticity and increases levels of synaptic proteins such as PSD95, GluA1, and Synapsin (Fogaca et al., 2019).

We have previously investigated the neuroprotective effects of a traditional Tibetan medicine called *Wangla*, the dried rhizome of *Coeloglossum viride* var. *bracteatum*, known for its antioxidant and anti-inflammatory effects in Xizang. In models of neurodegenerative diseases such as Alzheimer's disease and Parkinson's disease, *Coeloglossum viride* var. *bracteatum* extract (CE) has been shown to alleviate memory decline and motor dysfunction *in vivo* (Lang et al., 2022; Li, Cai, et al., 2021), and CE also inhibits inflammation and oxidative stress *in vitro* (Cai et al., 2021). Notably, our recent study found that CE inhibits the enhanced glycolytic activity on M1-type microglia and improves energy metabolism of M2-type microglia *in vitro*, suggests that CE has the potential to treat CNS disorders by inhibiting inflammation (Bai et al., 2023). Here, to investigate whether CE can inhibit MDD by suppressing inflammation, we constructed an LPS-induced acute depression model in mice and injected CE with CE. We first evaluated the construction of the MDD model and the inhibitory effect of CE on MDD by behavioral analysis. Then, we investigated the anti-inflammatory effect of CE, as well as its regulating effects on microglial energy metabolism, especially on the HIF-1 α /PKM2 axis of energy metabolism. Finally, we measured the effects of CE and LPS on dendritic spines and synaptic proteins to evaluate their influence on synaptic plasticity.

2. Material and methods

2.1. Animals

2-month-old C57BL/6J mice (males) were purchased from Beijing Vital River Laboratory Animal Technology Co., Ltd. under license No. SCXK (Beijing) 2021–0013. Mice were group-housed in a temperature-controlled room (22 °C) with a 12-h light/dark cycle and free access to water and food. The timeline of generating LPS-induced depressive-like model, CE administration, and behavioral experiments is shown in Fig. 1A.

The experimental protocol adhered to the guidelines of the Experimental Biology and Medical Ethics Review Committee of the Central University of Nationalities (ECMUC2019016AO). All efforts were made to minimize animal suffering and to reduce the number of animals used.

2.2. Chemicals and reagents

The preparation of *Coeloglossum viride* var. *bracteatum* extract (CE) and the identification of its constituents were carried out as previously described without modification (Cai et al., 2021). LPS was purchased from Sigma-Aldrich (#L2880).

2.3. Behavioral tests

Open field test (OFT): Mice were placed individually in a 50 × 50 cm² test box for 5 min and their movement trajectories were recorded with a camera. The total distance of the trajectories and the time spent in the central area were statistically analyzed using the BAS-100 Animal Behavior Analysis System (Chengdu Techman Software Co., Ltd, China) software.

Tail suspension test (TST): Mice were suspended by their tails using medical tape and kept hanging on the instrument for 6 min. For statistical analysis, the immobility time of each mouse was recorded during the last 5 min of the 6-minute test duration.

Forced swimming test (FST): Mice were trained to swim for 5 min the day before the test. For the swimming test, mice were placed in a glass cylinder (10 cm diameter) filled with 2.5 L of water for 6 min at 18–21 °C. For statistical analysis, the immobility time of each mouse for the last 5 min of the entire duration was recorded.

Sucrose preference test (SPT): Initially, mice were acclimatized to sucrose by providing two plain bottles containing sucrose/water (1:99,

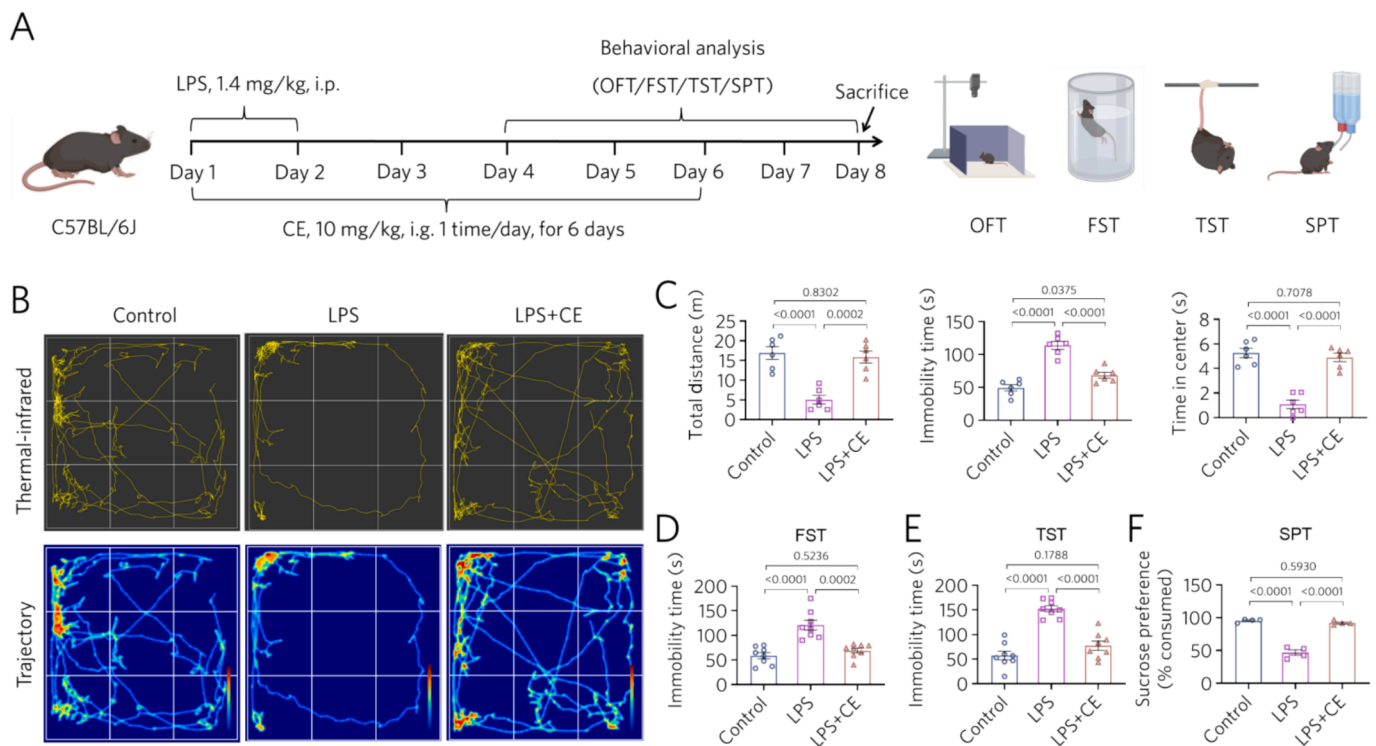


Fig. 1. CE alleviates LPS-induced depressive-like behaviors in mice. (A) Schematic diagram of experiments and behavioral tests. Mice were treated with LPS i.p. or CE i.g. followed by behavioral tests. (B) Representative trajectories and thermal-infrared images of mice in OFT. (C) Statistical analyses of the total distance, immobility time, and time in center of mice in the OFT ($n = 6$). (D) Immobility time of mice in FST ($n = 8$). (E) Immobility time of mice in the TST ($n = 8$). (F) Sucrose preference of mice in the SPT ($n = 4$). Differences between groups were analyzed by one-way ANOVA followed by Turkey's multiple comparisons test. The p -values are indicated on the graphs.

w/v) in their home cages. After 24 h of acclimatization, one bottle containing sucrose/water (1:99, w/v) and one bottle containing plain water were replaced, and the bottle positions were exchanged every 12 h. After 24 h of treatment, the remaining content in both bottles were calculated.

2.4. H&E staining

Hematoxylin-eosin (H&E) staining was employed to evaluate histological differences in liver, kidney, and lung. The staining procedure was conducted using the Hematoxylin and Eosin Staining Kit (Servicebio, #G1005) according to the manufacturer's protocol. Briefly, paraffin sections of organ tissues were heated at 60 °C for 30 min and then cooled to room temperature. These sections were then deparaffinised with xylene and washed with a gradient of ethanol of decreasing concentration. Subsequently, the sections were stained with hematoxylin, differentiated, blued, eosin stained, cleared and cover slipped. Finally, the mounts were observed using an upright microscope (BX53, Olympus, Japan).

2.5. Detection of serum transaminases and hormones

To evaluate liver inflammation, serum levels of two hepatic enzymes were analyzed: alanine aminotransferase (ALT) and glutamic oxaloacetic transaminase (GOT). ALT and GOT were detected using an Alanine Aminotransferase Assay Kit (#C009-2-1) and an Aspartate Aminotransferase Assay Kit (#C010-2-1), respectively, manufactured by Nanjing Jiancheng Bioengineering Institute.

Serum adrenocorticotropic hormone (ACTH) (#JL12373-48T), corticosterone (CORT) (#JL11918-48T) and corticotropin releasing hormone (CRH) (#JL11988-48T) were detected by ELISA kits supplied by Shanghai J&L Biotechnology Co. Ltd.

2.6. Detection of oxidative stress and inflammatory cytokines

Oxidative stress was evaluated in mouse brain using Superoxide Dismutase (SOD) Assay Kit (#A001-3-2), Catalase (CAT) Assay Kit (#A007-1-1), and Malondialdehyde (MDA) Assay Kit (#A003-1-2) from Nanjing Jiancheng Bioengineering Institute. Inflammatory cytokines in the mouse brain were determined using enzyme-linked immunosorbent assay (ELISA) kits, including TNF- α (#MM-0132M1), IL-1 β (#MM-0040M1), and IL-6 (#MM-0163M1) from Jiangsu Meimian Industrial Co., Ltd.

2.7. Immunofluorescence

Frozen brains were sectioned into 40 μ m slices at -20 °C using a cryostat microtome system (CM1860, Leica). For immunofluorescence staining, paraformaldehyde-fixed brain sections were rinsed three times with PBS and blocked with PBS containing 8 % goat serum, 0.4 % Triton X-100, 0.4 % Tween-20, 0.3 % glycine for 20 min at room temperature. After blocking, sections were rinsed three times with PBS and incubated with primary antibodies, IBA1 (1:500, Wako, #019-19741), iNOS (1:500, Santa Cruz Biotechnology, #sc-7271), and PKM2 (1:500, Proteintech, #60628-1-1g) overnight at 4 °C. Subsequently, the sections were incubated with secondary antibodies, Alexa Fluor 488-conjugated goat anti-rabbit IgG (H + L) (ZSGB-BIO, #ZF-0511) and Alexa Fluor 594-conjugated goat anti-mouse IgG (H + L) (ZSGB-BIO, #ZF-0513) for 2 h at room temperature. Cell nuclei were stained with DAPI. Images were acquired using a TCS SP8 confocal microscope (Leica, Germany).

2.8. Measurement of ATP, lactate, PK, HK, and PDH activities

ATP content in mouse brain was measured using ATP Assay Kit (Beyotime, #S0026). Lactate content was detected in mouse brain using

the Lactic Acid (LA) Content Assay Kit (Solarbio, #BC2235). In addition, Hexokinase (HK) Activity Assay Kit (#BC0745), Pyruvate Kinase (PK) Activity Assay Kit (#BC0545), and Pyruvate Dehydrogenase (PDH) Activity Assay Kit (#BC0385) were supplied by Beijing Solarbio Science & Technology Co., Ltd.

2.9. RT-qPCR

Total RNA was extracted from mouse hippocampus or hypothalamus using TRIzol Reagent (Invitrogen, #15596018CN), and 1 µg of RNA was used to generate cDNA using All-in-one 1st Strand cDNA Synthesis SuperMix (Novoprotein, #E047). Real-time PCR was performed in a Light Cycler 96 Real-Time PCR System (Roche) using 2× RealStar Fast SYBR qPCR Mix (GenStar, #A301-05). The primers sequences were as follows: *Glut1*, 5'-GCTTCTCCAACCTGACCTCAAAC-3' (sense) and 5'-ACGAGGAGCACCGTGAAGATGA-3' (anti-sense); *Hk2*, 5'-CCCTGTGAA-GATGTTGCCACT-3' (sense) and 5'-CCTTCGCTTGCCATTACGCAGC-3' (anti-sense); *Pkm2*, 5'-CAGAGAAGTCTTCTGGCTCA-3' (sense) and 5'-GCCACATCACTGCCTTCAGCAC-3' (anti-sense); *Ldha*, 5'-ACGCAGCAAGGAGCAGTGGAA-3' (sense) and 5'-ATGCTCTCAGC-CAAGTCTGCCA-3' (anti-sense); *G6pdx*, 5'-GACCAAGAAGC.

CTGGCATGTTTC-3' (sense) and 5'-AGACATCCAGGATGAGGCGTTC-3' (anti-sense); *Hif1α*, 5'-CTGCCACTGCCACCAACTG-3' (sense) and 5'-TGCCACTGTATGCTGATGCCTTAG-3' (anti-sense); Corticotropin-releasing factor receptor 1 (*Crrh1*), 5'-GGGAGCCCGTGTGAATTATT-3' (sense) and 5'-ATGACGGCAATGTGGTAGTGC-3' (anti-sense); Glucocorticoid receptor (*GR*) (*Nr3c1* in mouse), 5'-TGGAGAGGACAACCTGACTTCC-3' (sense) and 5'-ACGGAGGAGAACTCACATCTGG-3' (anti-sense).

2.10. Western blotting

Proteins were extracted by homogenizing dissected HIP and PFC and then concentration quantified using the BCA Protein Assay Kit (Beyotime, #P0011). Equal amounts of protein were loaded onto SDS-PAGE and transferred to a PVDF membrane. After blocking with 5 % skimmed milk, the membranes were incubated with primary antibodies at 4 °C, respectively, including HIF-1α (1:2000, Proteintech, #20960-1-AP), PKM2 (1:5000, Proteintech, #60268-1-Ig) and IBA1 (1:1000, Proteintech, #10904-1-AP), MAP2 (1:1000, Proteintech, #17490-1-AP), SYP (1:1000, Beyotime, #AF8091), PSD95 (1:1000, Proteintech, 20665-1-AP), β-actin (1:10,000, Proteintech, #81115-1-RR). Then secondary antibodies, including Dylight 800-Goat Anti-Rabbit IgG (1:10,000, Biodragon-Immunotech Co., Ltd., #BD9008), and Dylight 680-Goat Anti-Mouse IgG (1:10,000, Biodragon-Immunotech Co., Ltd., #BD9005) were incubated with the membranes for 1 h at room temperature. Protein blots were detected using the Odyssey CLx infrared fluorescence imaging system (LI-COR Biosciences). Relative protein levels were normalized using β-actin and quantified using Image J software (National Institutes of Health, Bethesda, MD, USA).

2.11. Immunohistochemistry

Paraffin-embedded mouse brain sections were de-paraffinized by xylene washes (xylene I, II, and III) followed by graded dehydration in an ethanol series and rinsed with distilled water. The sections were then immersed in citric acid buffer (pH 6.0) for antigen retrieval. After repair, sections were rinsed three times with PBS, blocked with 3 % BSA, and incubated with primary antibody MAP2 (1:100, Proteintech, #17490-1-AP) at 4 °C overnight. Sections were then incubated with HRP-conjugated secondary antibody, rinsed three more times with PBS, stained with DAB, counterstained with hematoxylin, and dehydrated. Eventually, the mounted sections were observed under a microscope (NIKON DS-U3) and positive cells were counted using Image-Pro Plus 6.0 software (Media Cybernetics, Inc.).

2.12. Golgi staining

Golgi staining was performed using the FD Rapid GolgiStain Kit (FD NeuroTechnologies, #PK401) according to the manufacturer's protocol and dendritic spine density was analyzed using Image J software.

2.13. Statistical analysis

Results are presented as mean ± S.E.M. Differences between groups were determined by one-way analysis of variance (ANOVA) followed by Turkey's multiple comparison tests in GraphPad Prism 9.0 software. The *p* values are shown numerically in the graphs.

3. Results

3.1. CE attenuated LPS-induced depressive-like behavior in mice

To evaluate the establishment of mouse model and investigate whether CE could rescue depressive-like behaviors, we divided the mice into three groups: 1) control group; 2) LPS group; and 3) LPS + CE group, with each contains eight mice. The control group received saline intraperitoneal injection for 6 days, while the LPS group received LPS at a dose of 1.4 mg/kg intraperitoneally for 2 days. Meanwhile, the LPS + CE group received a similar dose of LPS (1.4 mg/kg) intraperitoneally for 2 days followed by oral gavage of CE (10 mg/kg body weight) for 6 days (Fig. 1A). The progress of depressive-like behaviors was examined by open field test (OFT), forced swimming test (FST), tail suspension test (TST), and sucrose preference test (SPT) (Fig. 1B). In the OFT, mice receiving LPS displayed lower willingness to move (Fig. 1C–D). In contrast, we found no differences in time in center and total distance between mice in the LPS + CE group and control mice. LPS-induced depressive-like behaviors in mice were manifested by increased immobility time in TST (Fig. 1E) and FST (Fig. 1F) compared to the control group, which was effectively inhibited by CE at a dose of 10 mg/kg. In the SPT, mice receiving LPS had a lower preference for sucrose than controls, whereas mice in the LPS + CE group had a similar preference for sucrose as controls (Fig. 1G). These results suggest that CE significantly improves LPS-induced depressive-like behaviors, as evidenced by an increase in sucrose preference (SPT) and a decrease in immobility time in both the TST and FST (*p* < 0.05 in all comparisons).

3.2. CE ameliorated LPS-induced multi-organ damage in mice

To investigate the potential of CE in mitigating LPS-induced multi-organ damage, we assessed systemic inflammation by H&E staining of liver, kidney and lung tissues, and neuroinflammation by oxidative stress markers and cytokine levels in brain tissue. The results suggest that multiple inflammatory responses following exposure to LPS resulted in organ-specific damage, particularly in liver, kidney and lung tissues (Fig. 2A). In the liver tissues of LPS-treated mice, a marked transformation of macrophages into pro-inflammatory cells was observed, accompanied by the alteration of hepatocytes into ballooning cells (Fig. 2B), indicative of ballooning degeneration. Similarly, in the kidney tissues of LPS-treated mice, the tubular epithelial cells were swollen, resulting in narrowing of the inter-tubular spaces and extensive renal hemorrhage. Moreover, lung tissues from LPS-treated mice exhibited significant inflammatory cell infiltration and hemorrhage, along with alveolar exudation, leading to a reduction in the number of alveoli through the lung tissue (Fig. 2B). Collectively, these findings confirm that LPS promotes systemic inflammation and organ-specific responses. However, subsequent treatment with CE restored homeostasis in the liver, kidney, and lung tissues, demonstrating that CE is capable of mitigating LPS-induced damage in multiple organs in mice. Also, serum analyses revealed that mice in the LPS group exhibited significantly higher levels of ALT and GOT activities compared to their control counterparts (Fig. 2C). Notably, CE considerably decreased these

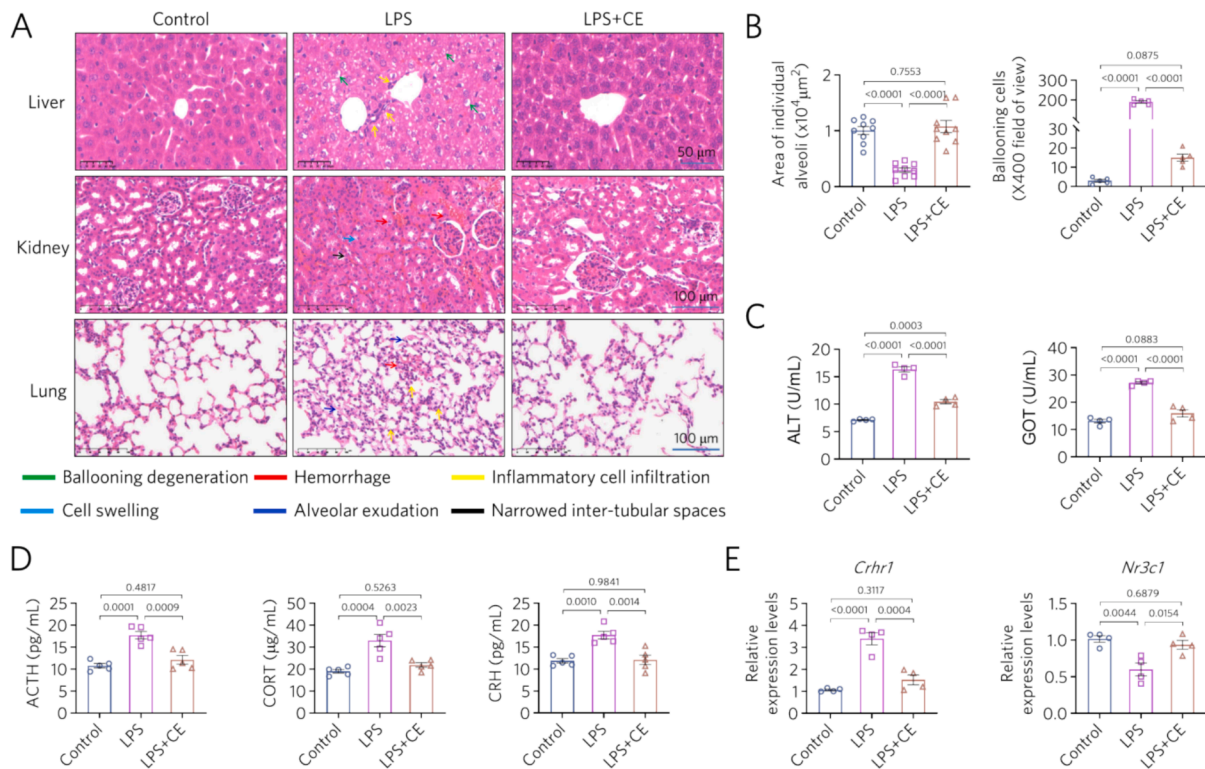


Fig. 2. CE ameliorates LPS-induced multi-organ inflammation in mice. (A) Representative images of H&E staining of liver, kidney, and lung. The original scale bar is shown in the lower left of each image, and the clearer remade scale bar is shown in the lower right. Colored arrows represent the different inflammatory status, and relevant explanations are listed below the images. (B) With LPS stimuli, hepatocytes were transformed into ballooning cells (left), and alveoli in lung were shrunken (right), whereas CE inhibited these effects of LPS (n = 5). (C) LPS increased the levels of alanine aminotransferase (ALT) and glutamic oxaloacetic transaminase (GOT) in blood, whereas CE decreased this increase (n = 4). (D) Serum ACTH, CORT, and CRH levels were measured by ELISA kits (n = 5). (E) Gene expression levels of *Crhr1* (Corticotropin-releasing factor receptor 1 gene) and *Nr3c1* (Glucocorticoid receptor gene) in the hypothalamus were examined by RT-qPCR (n = 4). Differences between groups were analyzed by one-way ANOVA followed by Turkey's multiple comparisons test, the p values were indicated.

elevations, underscoring its capacity to protect liver function.

Not only that, but we also tested the classical hypothalamic–pituitary–adrenal axis (HPA axis) hormones associated with depression. We found that serum levels of ACTH, CORT and CRH were elevated in LPS-treated mice (Fig. 2D). However, the concentrations of CRH, ACTH, and CORT were significantly lower in the CE-treated group (LPS + CE) mice (Fig. 2D). Correspondingly, the gene expression levels of two hormone receptors, *Crhr1* (Corticotropin-releasing factor receptor 1 gene) and *Nr3c1* (Glucocorticoid receptor gene), in the hypothalamus can also be regulated by CE. That is, LPS up-regulated the gene expression of the *Crhr1* while down-regulating the gene expression of *Nr3c1*, and CE could correct this change (Fig. 2E). This suggests that CE can regulate the levels of HPA axis-related hormones, i.e., CE may inhibit HPA axis hyperfunction by suppressing elevated serum concentrations of CRH, ACTH, and CORT, thereby improving the depression-like behavior of mice.

3.3. CE reduced LPS-induced neuroinflammation in mice

To determine whether CE prevents LPS-induced neuroinflammation in mice, we examined the inflammatory response in mouse brain. First, we quantified oxidative stress by measuring SOD and CAT activities and MDA content indicator. Compared with the control and LPS + CE groups, SOD and CAT activities were significantly lower in the LPS group, whereas MDA levels were elevated, indicating increased oxidative stress (Fig. 3A). Second, we evaluated change in inflammation-related factors. Pro-inflammatory cytokines (including TNF- α , IL-1 β , and IL-6) were significantly elevated in the LPS-treated group compared with the control group (Fig. 3B). Meanwhile, CE significantly reduced the production of pro-inflammatory cytokines. These results are

consistent with previous findings in LPS-induced MDD models (Li, Ali, et al., 2021; Miller & Raison, 2016; Peng et al., 2021), in which observed increased ROS production, lipid peroxidation, and cytokine release were observed. However, whether microglia are activated to a pro-inflammatory (M1) or anti-inflammatory (M2) phenotype remains unknown, as switching between M1-type microglia and M2-type microglia leads to different outcomes (Zhang et al., 2018). We co-stained the microglial marker IBA1 and M1 phenotype marker iNOS in the hippocampal CA1 and dentate gyrus (DG) regions as well as in the prefrontal cortex (PFC). In the LPS-treated group, co-localization of IBA1 and iNOS was observed, and microglia increased in size and decreased in branching, suggesting a shift to M1 phenotype after LPS stimulation (Fig. 3C–D). Nevertheless, CE effectively prevented microglia activation and transformation to the M1 phenotype. These results suggest that CE inhibits LPS-mediated microglial over-activation.

3.4. CE may inhibit aerobic glycolysis in M1-type microglia by restraining the HIF-1 α /PKM2 axis

Our previous study suggested that CE inhibited the aerobic glycolysis and improved OXPHOS in M1-type microglia *in vitro* by inhibiting the HIF-1 α /PKM2 signaling axis (Bai et al., 2023). As the co-staining of IBA1 and iNOS showed that, CE suppressed activation of M1-type microglia by down-regulating the activities of glycolytic enzymes (PK and HK) and up-regulating PDH, thus promoting a shift towards oxidative phosphorylation (OXPHOS). Compared with controls, the LPS group exhibited greater ATP consumption and lactate accumulation, which were end production of aerobic glycolysis (Fig. 4A). Furthermore, we measured the activities of PK and HK, which are crucial kinases in lactate production and the tricarboxylic acid cycle. The results were

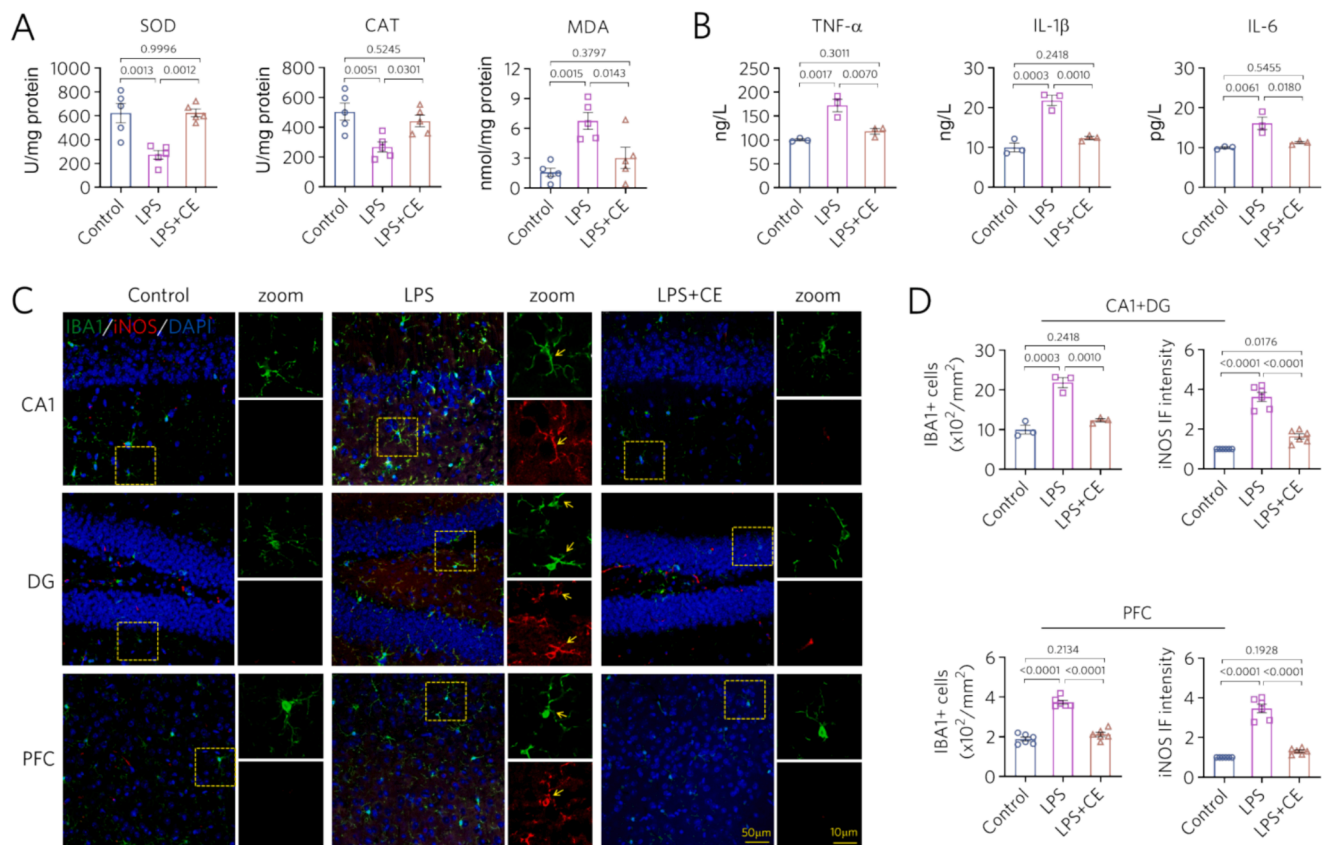


Fig. 3. CE reduces LPS-induced oxidative stress, neuroinflammation, and activation of M1-type microglia. (A) LPS activated oxidative stress in brain tissues, whereas CE reduced activation ($n = 5$). (B) LPS stimulated pro-inflammatory factors release in brain, which is inhibited by CE ($n = 3$). (C) Representative images of immunofluorescent staining of IBA1 (green) and iNOS (red) in hippocampal CA1 and dentate gyrus (DG), as well as the prefrontal cortex (PFC). (D) Number of IBA1 positive cells and relative iNOS immunofluorescent intensity in stained areas (hippocampal CA1 and DG on the left and PFC on the right) ($n = 6$). Data are expressed as mean \pm S.E.M and analyzed by one-way ANOVA and Turkey's multiple comparisons test, with the p -values marked in the graphs.

consistent with the observed changes in lactate levels. In addition, the activity of PDH, a key rate-limiting enzyme of acetyl-CoA generation, was down-regulated after exposure to LPS. However, there were not significant differences in energy metabolism indices between the CE-treated group and control groups. These results supported that LPS enhanced aerobic glycolysis, whereas CE suppressed the enhancement and facilitate the switch to OXPHOS.

To further validate the effect of CE on metabolic pathways, we investigated the expression of genes related to the metabolic transition from aerobic glycolysis to OXPHOS. Consistent with our previous findings (Bai et al., 2023), we examined the expression levels of glycolysis-related genes such as hypoxia inducible factor-1 α (*Hif1 α*), glucose transporter protein 1 (*Glut1*), hexokinase 2 (*Hk2*), M2-type pyruvate kinase (*Pkm2*), lactate dehydrogenase A (*Ldha*), and glucose 6-phosphate 1-dehydrogenase \times (*G6pdx*) using RT-qPCR. The expression of these genes was elevated under LPS stimulation, which was reversed by CE treatment (Fig. 4B).

PKM2 has been reported to irreversibly catalyze the conversion of phosphoenolpyruvate to pyruvate (Lynch, 2020), and HIF-1 α enhances this process by activating lactate dehydrogenase A (LDHA) (Tannahill et al., 2013), which increase lactate production and facilitates aerobic glycolysis in M1-type microglia. To elucidate the antidepressant mechanism of CE, we performed co-staining for PKM2 and IBA1 in HIP and PFC of brain slices. We found that PKM2 was highly expressed in LPS-stimulated M1-type microglia, whereas CE inhibited M1-type activation as well as PKM2 expression (Fig. 4C–D). Quantitative analysis of microglial morphology (including cell body size, branch number, and total branch length, confirmed that CE effectively inhibited the activation of M1-type microglia (Fig. 4E). Additionally, western blotting

analysis demonstrated that HIF-1 α had a similar trend with PKM2 (Fig. 4F–G). Thus, these results suggest that LPS triggers the activation of the HIF-1 α /PKM2 axis, resulting in aerobic glycolysis, and that administration of CE effectively inhibits this activation.

3.5. CE repaired LPS-induced neuronal loss and synaptic disruption

Dysfunction of microglial energy metabolism leads to abnormal cellular function and metabolism, interfering synaptic plasticity by altering morphology and synapse numbers (Cao et al., 2021; Gundersen, Storm-Mathisen, & Bergersen, 2015). Meanwhile, reductions in synapses and neurons have also been observed in MDD (Parekh et al., 2022; Price & Drevets, 2010). To determine whether CE regulation of microglia energy metabolism would be involved in maintaining neuronal survival and synaptic plasticity, we performed immunohistochemistry using the neuronal marker MAP2 and Golgi staining to assess dendritic spines. We observed obvious neuronal loss in the CA1 region and PFC after a single injection of LPS (Fig. 5A), and the count of MAP2 positive cells was consistent with the immunohistochemistry images (Fig. 5B). Conversely, CE prevented LPS-induced neuronal reduction. Besides, Golgi staining indicated a decrease in dendritic spine density in the CA1 region of the LPS group, which was align with previous findings (Fig. 5C) (Zhang et al., 2024). CE ameliorated the LPS-induced decreases in dendritic spine density and synaptic protein levels (SYP, PSD95), which supports an improvement in synaptic plasticity, and may underlie the observed behavioral improvements. Moreover, to elucidate the mechanisms of the reparative effects of CE, we analyzed the expression of two key proteins in pre- and postsynaptic formation, namely, the presynaptic synaptophysin (SYP) and postsynaptic marker PSD95. The

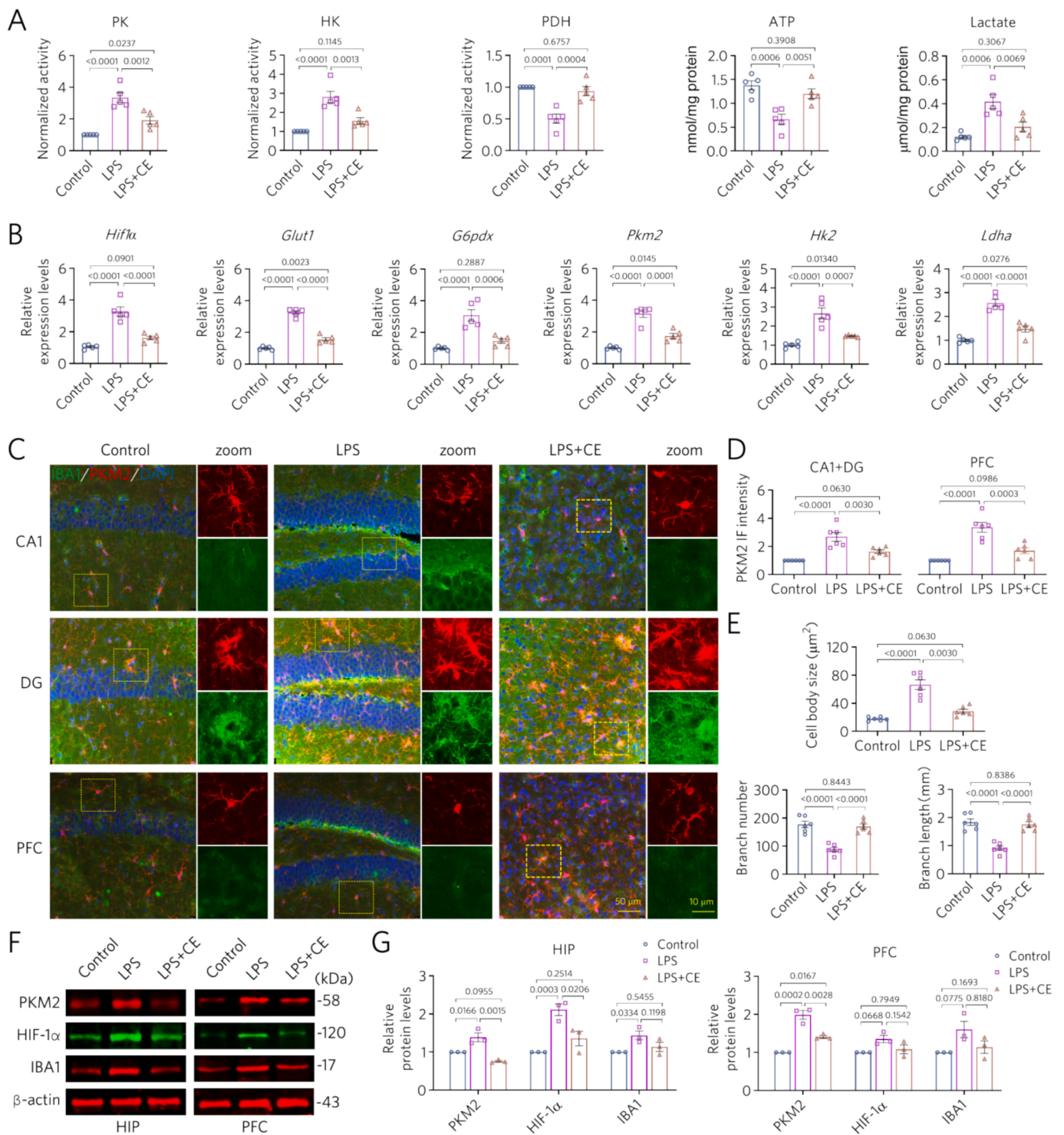


Fig. 4. CE inhibited LPS-induced enhancement of M1-type microglial aerobic glycolysis by restraining HIF-1α/PKM2 axis. (A) Measurement of the activities of HK, PK and PDH as well as ATP and lactate production (n = 5). (B) RT-qPCR for gene expression levels of *Hif1α*, *Glut1*, *G6pdx*, *Hk2*, *Pkm2*, and *Ldha* (n = 5). (C) Representative images of immunofluorescence staining for IBA1 (red) and PKM2 (green) in hippocampal CA1, dentate gyrus (DG) and prefrontal cortex (PFC). (D) Relative values of PKM2 immunofluorescence intensity in the stained regions (hippocampal CA1 and DG on the left, PFC area on the right) (n = 6). (E) Quantitative analysis of the cell body size, number of branches and total branch length of microglia (n = 6). (F-G) Western blotting and quantitative analysis of PKM2, HIF-1α and IBA1 protein levels of in hippocampus (HIP) and PFC (n = 3). Relative expression levels were standardized to β-actin. In this figure, differences between groups were analyzed by one-way ANOVA followed by Turkey's multiple comparisons test. The p-values were marked.

levels of SYP and PSD95 were elevated in the CE-treated group compared with that of the LPS group (Fig. 5D). Together, these data suggest that CE can repair LPS-induced neuronal loss and disruption of synaptic plasticity.

4. Discussion

The relationship between neuroinflammation and depression is a compelling area of research. Since the 1990s, it has been recognized that

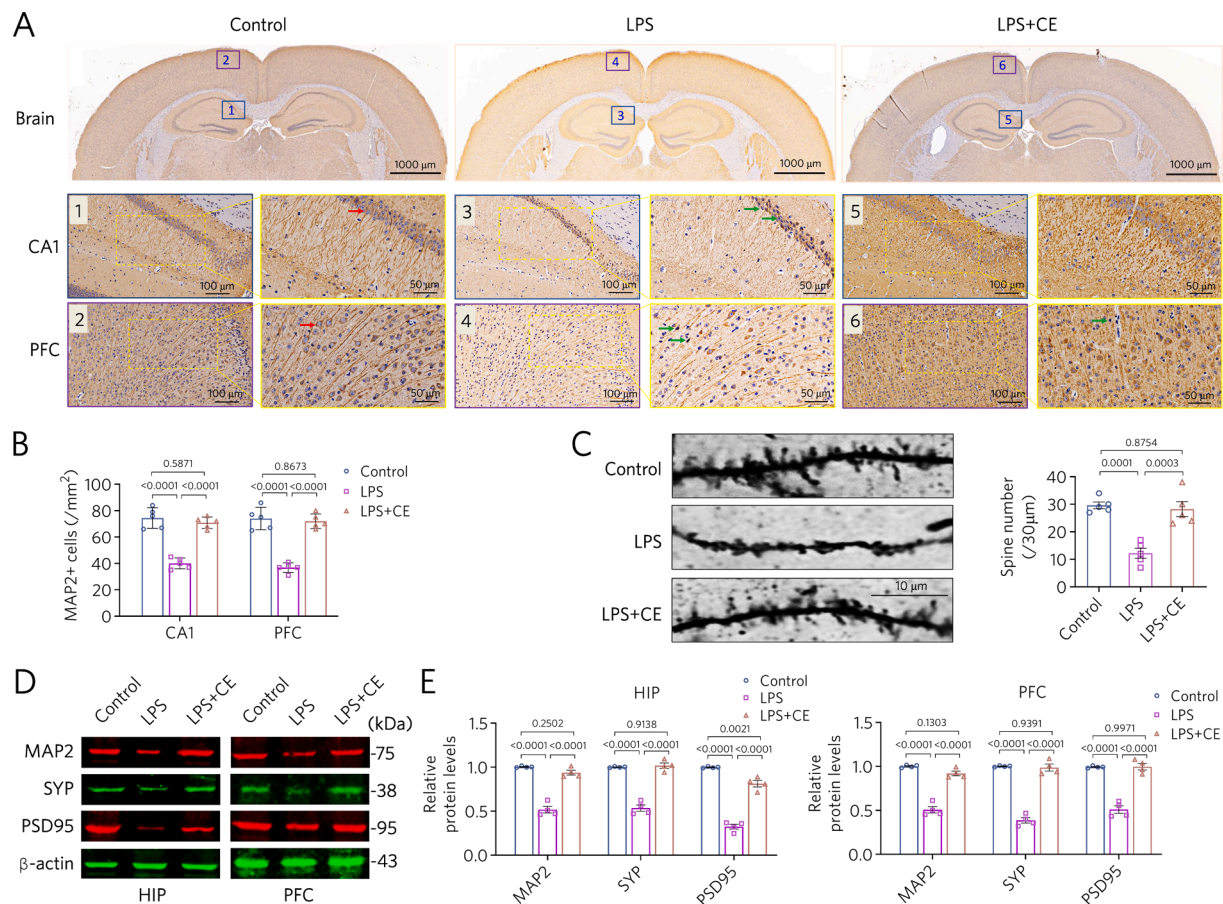


Fig. 5. CE prevents LPS-induced neuronal loss and synaptic disruption. (A) Representative images of immunohistochemistry staining of MAP2 positive cells (indicates neurons) in hippocampal CA1 and prefrontal cortex (PFC) regions. (B) Number of MAP2 positive cells in the stained areas (hippocampal CA1 and PFC) ($n = 5$). (C) Representative images of Golgi-stained dendrites in the HIP-CA1 area and quantification of the number of spines ($n = 5$). (D) Western blotting and quantitative data of MAP2, SYP and PSD95 protein levels in hippocampus (HIP) and PFC ($n = 4$). Relative expression levels were normalized to β -actin. Data are shown as mean \pm S.E.M and were analyzed by one-way ANOVA with Turkey's multiple comparisons test. The p -values were indicated.

psychological stress triggers immune activation and that an increase in inflammatory cytokines can lead to depression (Bierhaus et al., 2003). As a result, the "neuroinflammatory hypothesis" was subsequently proposed (Smith, 1991). Neuroinflammation and metabolic alterations in microglia have been previously reported in MDD (Miller & Raison, 2016). As immune cells in the CNS, microglia play a key role in maintaining brain homeostasis (Hemonnot, Hua, Ulmann, & Hirbec, 2019). In pathological situations, microglia shift from a quiescent to an activate state, displaying immune responses including migration, phagocytosis, and releasing inflammatory cytokines (Sierra, Paolicelli, & Kettenmann, 2019). In these processes, microglia are a major source of inflammatory cytokines, and their hyperactivation mediates neuroinflammation, resulting in multiple neurological disorders. Microglia can be polarized into two phenotypes: the M1 phenotype promotes inflammation, contributing to the pathogenesis of MDD as well as neuronal and synaptic dysfunction, and the M2 phenotype supports neuroprotection and brain repair (Wake, Horiuchi, Kato, Moorhouse, & Nabekura, 2019; Zhang et al., 2024). Reducing neuroinflammation and altering the balance of microglia M1/M2 phenotype polarization has been reported to ameliorate depressive-like behaviors in mice exposed to chronic unpredictable stress (Liu et al., 2024), highlighting the therapeutic potential of targeting microglial phenotype switching in anti-depression strategies. Here, we demonstrate that CE ameliorates LPS-induced MDD phenotype and systemic damage, including suppression of the onset of depressive-like behaviors, reducing systemic inflammation, and curbing neuroinflammation. Increased inflammatory stimuli drive the conversion of activated microglia to an M1-type, which is reversed by CE

through modulating aerobic glycolysis to OXPHOS. In addition, CE increases the expression of synaptic proteins SYN and PSD95, and increases dendritic spines, which are associated with synaptic formation and function.

LPS is widely used to construct models of inflammation. During LPS stimuli, increases in inflammatory cytokines such as TNF- α , IL-6, and IL-1 β drive the pathogenesis of depression (Enache et al., 2019; Shapouri-Moghaddam et al., 2018; Yin et al., 2023). LPS-induced systemic inflammatory response syndrome (SIRS) is known to cause significant damage to the liver, kidney, and lung. It is widely accepted that LPS does not act primarily by crossing the blood-brain barrier (BBB), but by inducing CNS inflammation through inflammatory signals generated by peripheral tissues. Our data showed that CE has a significant protective effect against LPS-induced liver injury. However, we could not conclusively determine whether this neuroprotective effect acts through the liver-brain axis. Our data also show that in addition to increased inflammatory cytokines, LPS also resulted in oxidative stress in HIP and PFC. In line with existing antidepressant candidate studies, CE was effective in mitigating these inflammatory responses. We also found that inflammatory stimuli induced microglia activation. Hyperactivation of microglia has been reported to promote neuroinflammation in turn, depending on the phenotype of microglia (Zhang et al., 2018). M1-type microglia releases pro-inflammatory cytokines, whereas M2-type microglia releases anti-inflammatory cytokines. We found significant difference in the number of inactivated microglia and M1 phenotype microglia between the LPS and CE-treated groups. With LPS stimuli, massive microglia were activated and transformed to M1-type

microglia, consistent with previous studies. CE inhibited the over-activation of microglia, especially M1-type microglia, consistent with inflammatory cytokine levels. These findings indicate that CE exerts anti-depression effects by regulating M1 polarization of microglia (Fig. 6).

The metabolic flexibility in microglia has emerged as a novel target for the treatment of CNS diseases, with a particular focus on the metabolic shift between aerobic glycolysis and OXPHOS (Ghosh et al., 2018; Gundersen et al., 2015; Pan et al., 2022). The switch from aerobic glycolysis to OXPHOS is a hallmark of inflammatory activation in microglia, which has been reported to be reversed by eliminating the NLR Family Pyrin Domain Containing 3 (NLRP3) inflammasome or inhibiting NF- κ B pathway (Arioz et al., 2019; Cheng et al., 2021; Zhang et al., 2024). Our previous study proposed that CE could inhibit the aerobic glycolysis in M1-type microglia by inhibiting HIF-1 α /PKM2 signaling axis (Bai et al., 2023). The present study further revealed that CE could prevent microglia activation, particularly in the M1-type, by down-regulating two key enzymes (PK and HK) in the aerobic glycolysis pathway and up-regulating PDH, pivotal for OXPHOS. These results indicate that CE transformed the energy metabolism of M1-type microglia from aerobic glycolysis to OXPHOS. Furthermore, CE inhibited the activation of HIF-1 α /PKM2 signaling axis. The combination of PKM2 and HIF-1 α is considered to activate macrophages toward the M1-type, contributing to transcription of glycolytic genes and eventually aerobic glycolysis process (Ouyang et al., 2018). We also found that *Glut1* expression levels were down-regulated in the LPS group and up-regulated in the CE-treated group. *Glut1* has been reported to increase glucose uptake by microglia and promote the switch of OXPHOS to aerobic glycolysis, while *Glut1*-blocked microglia have lower glycolytic and phagocytic activity (Wang et al., 2019). These results strongly suggest that CE can alter microglia energy metabolism, resulting in visible effects on inflammation and MDD phenotypes.

The “inflammation-depression model” posits that infection-induced inflammation can lead to depression, at least in part, via the HPA axis (Dantzer, O'Connor, Freund, Johnson, & Kelley, 2008; Miller & Raison, 2016). However, previous studies using the LPS-induced depression

model have had inconsistent findings on changes in HPA axis hormone levels (Sun et al., 2023; Yu et al., 2022). Glucocorticoids are the most potent anti-inflammatory hormones in human body. Glucocorticoid receptor expression is reduced in both patients with MDD and in mouse models (Carvalho et al., 2014; Deng et al., 2019). This reduction leads to glucocorticoid resistance, an important biological abnormality observed in patients. Our findings suggest that CE mitigates the inflammation-induced decrease in GR expression and increase of CRHR1 expression. These results provide additional evidence for the efficacy of CE in addressing inflammation-induced depression.

Neuronal dysfunction and impaired synaptic plasticity are associated with MDD (Wohleb, Terwilliger, Duman, & Duman, 2018). Numerous studies have highlighted that reductions in synaptic proteins and dendritic spines are linked to cognitive and mental disorders (Kim et al., 2010; Parekh et al., 2022), as these elements are crucial for synapse formation, synaptic vesicle function, and neuronal activity. Consistently, SYN and PSD95 expression has been reported to be reduced in HIP, PFC and amygdala in various models of depression, and these changes can be reversed by antidepressants (Hao et al., 2024; Vatan-doust & Meftahi, 2022). A similar LPS-induced reduction was observed in our study. However, treatment with CE resulted in increased expression of SYN and PSD95 in the HIP and PFC regions, along with elevated dendritic spine density, thus supporting neuronal survival, as evidenced by the maintenance of the number of neurons labeled by MAP2 staining (Fig. 6). Our findings are in agreement with others, revealing the potential of CE as an antidepressant.

Despite the encouraging findings, there are some limitations to our study. This study is limited by its focus on acute LPS-induced MDD models. Future research should explore the long-term effects of CE in chronic depression models and investigate the role of CE in modulating other pathways involved in synaptic plasticity, such as the complement system. Recent studies have shown that inflammatory stimuli activate the complement pathway and increase the production of complement protein C3, which directly activates complement receptor 3 (CR3) on microglia, thereby contributing to synaptic elimination via phagocytosis (Stevens et al., 2007; Zhong et al., 2023). Through regulating the

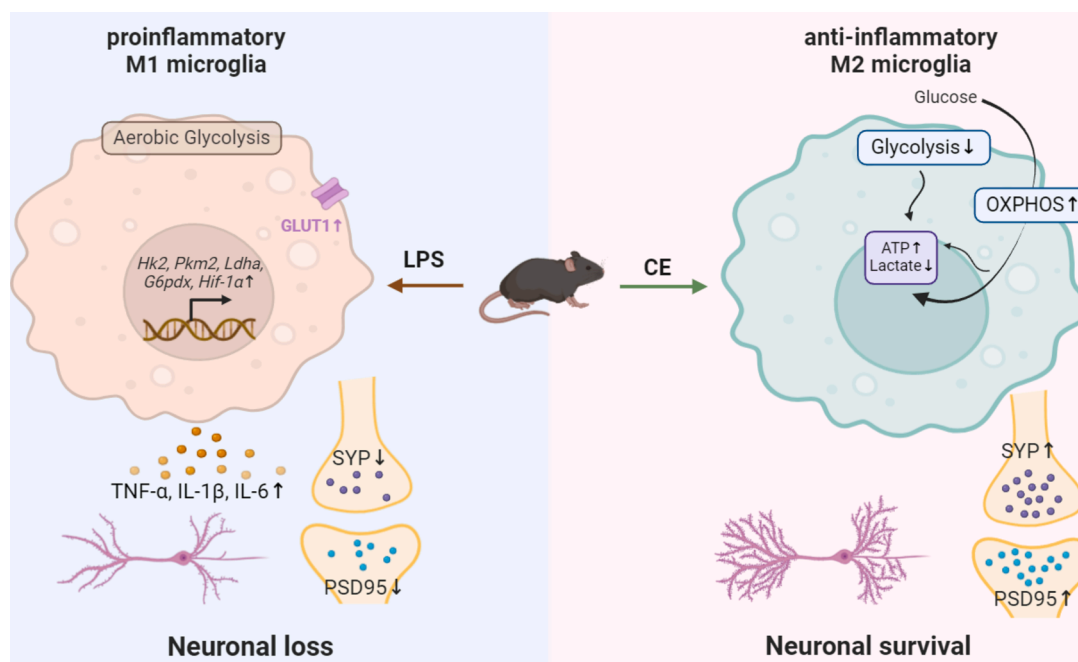


Fig. 6. CE inhibits neuronal loss and synaptic disruption, thereby attenuating LPS-induced depressive-like behavior in mice. CE ameliorated LPS-induced depressive phenotypes in mice. Consistent with the inhibitory effect on inflammation, CE reduced the levels of proinflammatory cytokines TNF- α , IL-1 β , IL-6 in the brain of LPS-injected mice. Mechanistically, CE altered the phenotypic polarization of microglia through inhibiting aerobic glycolysis but enhancing OXPHOS, thereby protecting against loss of synaptic proteins, dendritic spines, and neurons. The image was created with [BioRender.com](https://www.biorender.com) with agreement number: MS2710G7PX.

complement C3/CR3 pathway, it is possible to inhibit aberrant microglia-mediated synaptic pruning, thereby contributing to the alleviation of depressive symptoms (Hao et al., 2024). Our results suggest that CE may rescue the MDD phenotype by modulating microglia polarization through the inhibition of the HIF-1 α /PKM2 axis, reducing neuroinflammation, and enhancing synaptic plasticity. These results align with recent studies highlighting the therapeutic potential of targeting microglia metabolism and synaptic integrity in MDD. Thus, further studies are needed to investigate the role of CE in the regulation of the C3/CR3 pathway and its potential impact on depression.

5. Conclusion

We found that CE is beneficial in LPS-induced MDD in mice. These protective effects were achieved by inhibiting neuroinflammation, switching microglia phenotype by transforming aerobic glycolysis to OXPHOS, and repairing synaptic plasticity. These findings deepen our understanding of the medicinal value of CE and suggest new applications for it.

CRedit authorship contribution statement

The Guo: Methodology, Data curation. **Jinpeng Bai:** Writing – original draft, Visualization, Software, Formal analysis. **Jun Wang:** Investigation, Data curation. **Xiuyuan Lang:** Writing – original draft, Validation, Software. **Min-Min Cao:** Data curation, Software. **Si-Jia Zhong:** Writing – original draft, Visualization. **Liang Cui:** Validation, Software. **Yang Hu:** Writing – review & editing. **Xiao-Yan Qin:** Writing – original draft, Supervision, Project administration, Funding acquisition. **Rongfeng Lan:** Writing – review & editing, Supervision.

Declaration of competing interest

The authors declare that they have no known competing financial interests or personal relationships that could have appeared to influence the work reported in this paper.

Acknowledgements

This study is supported by the National Natural Science Foundation of China (81873088), research projects on traditional Chinese medicine by the Guangxi Administration of Traditional Chinese Medicine (No. 2024ZC2856). Thanks to Biorender (www.biorender.com) for granting publication and licensing rights (Agreement number MS2710G7PX).

Data availability

Data will be made available on request.

References

- Arioz, B. I., Tastan, B., Tarakcioglu, E., Tufekci, K. U., Olcum, M., Ersoy, N., ... Genc, S. (2019). Melatonin attenuates LPS-induced acute depressive-like behaviors and microglial NLRP3 inflammasome activation through the SIRT1/Nrf2 pathway. *Frontiers in Immunology*, 10, 1511. <https://doi.org/10.3389/fimmu.2019.01511>
- Bai, J.-P., Wang, J., Hu, Y., Huang, Q., Dai, J.-F., Xiao, G.-L., ... Lan, R. (2023). Network pharmacological analysis of the active molecules in *Coeloglossum viride* var. *bacteatum* and their anti-Alzheimer's disease activity through restoration of energy metabolism and inhibition of inflammation. *Arabian Journal of Chemistry*, 16(8). <https://doi.org/10.1016/j.arabjc.2023.105008>
- Bierhaus, A., Wolf, J., Andrassy, M., Rohleder, N., Humpert, P. M., Petrov, D., ... Nawroth, P. P. (2003). A mechanism converting psychosocial stress into mononuclear cell activation. *Proceedings of the National Academy of Sciences of the United States of America*, 100(4), 1920–1925. <https://doi.org/10.1073/pnas.0438019100>
- Burke, N. N., Kerr, D. M., Moriarty, O., Finn, D. P., & Roche, M. (2014). Minocycline modulates neuropathic pain behaviour and cortical M1–M2 microglial gene expression in a rat model of depression. *Brain, Behavior, and Immunity*, 42, 147–156. <https://doi.org/10.1016/j.bbi.2014.06.015>
- Cai, Z. P., Cao, C., Guo, Z., Yu, Y., Zhong, S. J., Pan, R. Y., ... Qin, X. Y. (2021). *Coeloglossum viride* var. *bacteatum* extract attenuates staurosporine induced neurotoxicity by restoring the FGF2-P13K/Akt signaling axis and Dnm3t. *Heliyon*, 7(7), e07503.
- Cao, P., Chen, C., Liu, A., Shan, Q., Zhu, X., Jia, C., ... Zhang, Z. (2021). Early-life inflammation promotes depressive symptoms in adolescence via microglial engulfment of dendritic spines. *Neuron*, 109(16), 2573–2589. <https://doi.org/10.1016/j.neuron.2021.06.012>
- Carvalho, L. A., Bergink, V., Sumaski, L., Wijkhuijs, J., Hoogendijk, W. J., Birkenhager, T. K., & Drexhage, H. A. (2014). Inflammatory activation is associated with a reduced glucocorticoid receptor alpha/beta expression ratio in monocytes of inpatients with melancholic major depressive disorder. *Translational Psychiatry*, 4(1), e344.
- Cheng, J., Zhang, R., Xu, Z., Ke, Y., Sun, R., Yang, H., ... Zheng, L. T. (2021). Early glycolytic reprogramming controls microglial inflammatory activation. *Journal of Neuroinflammation*, 18(1), 129. <https://doi.org/10.1186/s12974-021-02187-y>
- Cui, L., Li, S., Wang, S., Wu, X., Liu, Y., Yu, W., ... Li, B. (2024). Major depressive disorder: Hypothesis, mechanism, prevention and treatment. *Signal Transduction and Targeted Therapy*, 9(1), 30. <https://doi.org/10.1038/s41392-024-01738-y>
- Dantzer, R., O'Connor, J. C., Freund, G. G., Johnson, R. W., & Kelley, K. W. (2008). From inflammation to sickness and depression: When the immune system subjugates the brain. *Nature Reviews Neuroscience*, 9(1), 46–56. <https://doi.org/10.1038/nrn2297>
- Deng, X., Fu, J., Song, Y., Xu, B., Ji, Z., Guo, Q., & Ma, S. (2019). Glucocorticoid receptor dysfunction orchestrates inflammasome effects on chronic obstructive pulmonary disease-induced depression: A potential mechanism underlying the cross talk between lung and brain. *Brain, Behavior, and Immunity*, 79, 195–206. <https://doi.org/10.1016/j.bbi.2019.02.001>
- Enache, D., Pariante, C. M., & Mondelli, V. (2019). Markers of central inflammation in major depressive disorder: A systematic review and meta-analysis of studies examining cerebrospinal fluid, positron emission tomography and post-mortem brain tissue. *Brain, Behavior, and Immunity*, 81, 24–40. <https://doi.org/10.1016/j.bbi.2019.06.015>
- Felger, J. C., & Lotrich, F. E. (2013). Inflammatory cytokines in depression: Neurobiological mechanisms and therapeutic implications. *Neuroscience*, 246, 199–229. <https://doi.org/10.1016/j.neuroscience.2013.04.060>
- Fogaca, M. V., Fukumoto, K., Franklin, T., Liu, R. J., Duman, C. H., Vitolo, O. V., & Duman, R. S. (2019). N-Methyl-D-aspartate receptor antagonist d-methadone produces rapid, mTORC1-dependent antidepressant effects. *Neuropsychopharmacology*, 44(13), 2230–2238. <https://doi.org/10.1038/s41386-019-0501-x>
- Ghosh, S., Castillo, E., Frias, E. S., & Swanson, R. A. (2018). Bioenergetic regulation of microglia. *Glia*, 66(6), 1200–1212. <https://doi.org/10.1002/glia.23271>
- Gundersen, V., Storm-Mathisen, J., & Bergersen, L. H. (2015). Neuroglial transmission. *Physiological Reviews*, 95(3), 695–726. <https://doi.org/10.1152/physrev.00024.2014>
- Guo, S., Wang, H., & Yin, Y. (2022). Microglia polarization from M1 to M2 in neurodegenerative diseases. *Frontiers in Aging Neuroscience*, 14, Article 815347. <https://doi.org/10.3389/fnagi.2022.815347>
- Hao, W., Ma, Q., Wang, L., Yuan, N., Gan, H., He, L., ... Chen, J. (2024). Gut dysbiosis induces the development of depression-like behavior through abnormal synapse pruning in microglia-mediated by complement C3. *Microbiome*, 12(1), 34. <https://doi.org/10.1186/s40168-024-01756-6>
- Hemmonot, A. L., Hua, J., Ulmann, L., & Hirbec, H. (2019). Microglia in Alzheimer disease: well-known targets and new opportunities. *Frontiers in Aging Neuroscience*, 11, 233. <https://doi.org/10.3389/fnagi.2019.00233>
- Kim, H. W., Rapoport, S. I., & Rao, J. S. (2010). Altered expression of apoptotic factors and synaptic markers in postmortem brain from bipolar disorder patients. *Neurobiology of Disease*, 37(3), 596–603. <https://doi.org/10.1016/j.nbd.2009.11.010>
- Krishnan, V., & Nestler, E. J. (2008). The molecular neurobiology of depression. *Nature*, 455(7215), 894–902. <https://doi.org/10.1038/nature07455>
- Lang, X. Y., Hu, Y., Bai, J. P., Wang, J., Qin, X. Y., & Lan, R. (2022). *Coeloglossum viride* var. *bacteatum* extract attenuates MPTP-induced neurotoxicity in vivo by restoring BDNF-TrkB and FGF2-Akt signaling axis and inhibiting RIP1-driven inflammation. *Frontiers in Pharmacology*, 13, Article 903235. <https://doi.org/10.3389/fphar.2022.903235>
- Li, W., Ali, T., He, K., Liu, Z., Shah, F. A., Ren, Q., ... Li, S. (2021). Ibrutinib alleviates LPS-induced neuroinflammation and synaptic defects in a mouse model of depression. *Brain, Behavior, and Immunity*, 92, 10–24. <https://doi.org/10.1016/j.bbi.2020.11.008>
- Li, X. X., Cai, Z. P., Lang, X. Y., Pan, R. Y., Ren, T. T., Lan, R. F., & Qin, X. Y. (2021). *Coeloglossum viride* var. *bacteatum* extract improves cognitive deficits by restoring BDNF, FGF2 levels and suppressing RIP1/RIP3/MLKL-mediated neuroinflammation in a 5xFAD mouse model of Alzheimer's disease. *ARTN 104612 Journal of Functional Foods*, 85. <https://doi.org/10.1016/j.jff.2021.104612>
- Li, Z., Ruan, M., Chen, J., & Fang, Y. (2021). Major depressive disorder: advances in neuroscience research and translational applications. *Neuroscience Bulletin*, 37(6), 863–880. <https://doi.org/10.1007/s12264-021-00638-3>
- Liu, L., Tang, J., Liang, X., Li, Y., Zhu, P., Zhou, M., ... Tang, Y. (2024). Running exercise alleviates hippocampal neuroinflammation and shifts the balance of microglial M1/M2 polarization through adiponectin/AdipoR1 pathway activation in mice exposed to chronic unpredictable stress. *Molecular Psychiatry*. <https://doi.org/10.1038/s41380-024-02464-1>
- Lynch, M. A. (2020). Can the emerging field of immunometabolism provide insights into neuroinflammation? *Progress in Neurobiology*, 184, Article 101719. <https://doi.org/10.1016/j.pneurobio.2019.101719>
- Malhi, G. S., & Mann, J. J. (2018). Depression. *Lancet*, 392(10161), 2299–2312. [https://doi.org/10.1016/S0140-6736\(18\)31948-2](https://doi.org/10.1016/S0140-6736(18)31948-2)

- Marwaha, S., Palmer, E., Suppes, T., Cons, E., Young, A. H., & Uptegrove, R. (2023). Novel and emerging treatments for major depression. *Lancet*, 401(10371), 141–153. [https://doi.org/10.1016/S0140-6736\(22\)02080-3](https://doi.org/10.1016/S0140-6736(22)02080-3)
- Marx, W., Penninx, B., Solmi, M., Furukawa, T. A., Firth, J., Carvalho, A. F., & Berk, M. (2023). Major depressive disorder. *Nature Reviews Disease Primers*, 9(1), 44. <https://doi.org/10.1038/s41572-023-00454-1>
- Miller, A. H., Maletic, V., & Raison, C. L. (2009). Inflammation and its discontents: The role of cytokines in the pathophysiology of major depression. *Biological Psychiatry*, 65(9), 732–741. <https://doi.org/10.1016/j.biopsych.2008.11.029>
- Miller, A. H., & Raison, C. L. (2016). The role of inflammation in depression: From evolutionary imperative to modern treatment target. *Nature Reviews Immunology*, 16(1), 22–34. <https://doi.org/10.1038/nri.2015.5>
- Moda-Sava, R. N., Murdock, M. H., Parekh, P. K., Fetcho, R. N., Huang, B. S., Huynh, T. N., ... Liston, C. (2019). Sustained rescue of prefrontal circuit dysfunction by antidepressant-induced spine formation. *Science*, 364(6436). <https://doi.org/10.1126/science.aat8078>
- Nair, S., Sobotka, K. S., Joshi, P., Gressens, P., Fleiss, B., Thornton, C., ... Hagberg, H. (2019). Lipopolysaccharide-induced alteration of mitochondrial morphology induces a metabolic shift in microglia modulating the inflammatory response in vitro and in vivo. *Glia*, 67(6), 1047–1061. <https://doi.org/10.1002/glia.23587>
- Orihuela, R., McPherson, C. A., & Harry, G. J. (2016). Microglial M1/M2 polarization and metabolic states. *British Journal of Pharmacology*, 173(4), 649–665. <https://doi.org/10.1111/bph.13139>
- Ouyang, X., Han, S. N., Zhang, J. Y., Dioletis, E., Nemeth, B. T., Pacher, P., ... Mehal, W. Z. (2018). Digoxin suppresses pyruvate kinase M2-promoted HIF-1 α transactivation in steatohepatitis. *Cell Metabolism*, 27(2), 339–350 e333. <https://doi.org/10.1016/j.cmet.2018.01.007>
- Pan, R. Y., He, L., Zhang, J., Liu, X., Liao, Y., Gao, J., ... Yuan, Z. (2022). Positive feedback regulation of microglial glucose metabolism by histone H4 lysine 12 lactylation in Alzheimer's disease. *Cell Metabolism*, 34(4), 634–648 e636. <https://doi.org/10.1016/j.cmet.2022.02.013>
- Parekh, P. K., Johnson, S. B., & Liston, C. (2022). Synaptic mechanisms regulating mood state transitions in depression. *Annual Review of Neuroscience*, 45, 581–601. <https://doi.org/10.1146/annurev-neuro-110920-040422>
- Peng, Z., Li, X., Li, J., Dong, Y., Gao, Y., Liao, Y., ... Cheng, J. (2021). Dlg1 knockout inhibits microglial activation and alleviates lipopolysaccharide-induced depression-like behavior in mice. *Neuroscience Bulletin*, 37(12), 1671–1682. <https://doi.org/10.1007/s12264-021-00765-x>
- Price, J. L., & Drevets, W. C. (2010). Neurocircuitry of mood disorders. *Neuropsychopharmacology*, 35(1), 192–216. <https://doi.org/10.1038/npp.2009.104>
- Sakrajda, K., & Szczepankiewicz, A. (2021). Inflammation-related changes in mood disorders and the immunomodulatory role of lithium. *International Journal of Molecular Sciences*, 22(4). <https://doi.org/10.3390/ijms22041532>
- Schnieder, T. P., Trencavska, I., Rosoklija, G., Stankov, A., Mann, J. J., Smiley, J., & Dwork, A. J. (2014). Microglia of prefrontal white matter in suicide. *Journal of Neuropathology and Experimental Neurology*, 73(9), 880–890. <https://doi.org/10.1097/NEN.0000000000000107>
- Shapouri-Moghaddam, A., Mohammadian, S., Vazini, H., Taghadosi, M., Esmaili, S. A., Mardani, F., ... Sahebkar, A. (2018). Macrophage plasticity, polarization, and function in health and disease. *Journal of Cellular Physiology*, 233(9), 6425–6440. <https://doi.org/10.1002/jcp.26429>
- Sierra, A., Paolicelli, R. C., & Kettenmann, H. (2019). Cien Anos de Microglia: Milestones in a century of microglial research. *Trends in Neurosciences*, 42(11), 778–792. <https://doi.org/10.1016/j.tins.2019.09.004>
- Smith, R. S. (1991). The macrophage theory of depression. *Medical Hypotheses*, 35(4), 298–306. [https://doi.org/10.1016/0306-9877\(91\)90272-z](https://doi.org/10.1016/0306-9877(91)90272-z)
- Stevens, B., Allen, N. J., Vazquez, L. E., Howell, G. R., Christopherson, K. S., Nouri, N., ... Barres, B. A. (2007). The classical complement cascade mediates CNS synapse elimination. *Cell*, 131(6), 1164–1178. <https://doi.org/10.1016/j.cell.2007.10.036>
- Sun, J., Qiu, L., Zhang, H., Zhou, Z., Ju, L., & Yang, J. (2023). CRHR1 antagonist alleviates LPS-induced depression-like behaviour in mice. *BMC Psychiatry*, 23(1), 17. <https://doi.org/10.1186/s12888-023-04519-z>
- Tannahill, G. M., Curtis, A. M., Adamik, J., Palsson-McDermott, E. M., McGettrick, A. F., Goel, G., ... O'Neill, L. A. (2013). Succinate is an inflammatory signal that induces IL-1 β through HIF-1 α . *Nature*, 496(7444), 238–242. <https://doi.org/10.1038/nature11986>
- Vatandoust, S. M., & Meftahi, G. H. (2022). The effect of sericin on the cognitive impairment, depression, and anxiety caused by learned helplessness in male mice. *Journal of Molecular Neuroscience*, 72(5), 963–974. <https://doi.org/10.1007/s12031-022-01982-3>
- Wake, H., Horiuchi, H., Kato, D., Moorhouse, A. J., & Nabekura, J. (2019). Physiological implications of microglia-synapse interactions. *Methods in Molecular Biology*, 2034, 69–80. https://doi.org/10.1007/978-1-4939-9658-2_6
- Walker, D. J., & Spencer, K. A. (2018). Glucocorticoid programming of neuroimmune function. *General and Comparative Endocrinology*, 256, 80–88. <https://doi.org/10.1016/j.ygcen.2017.07.016>
- Wang, L., Pavlou, S., Du, X., Bhukory, M., Xu, H., & Chen, M. (2019). Glucose transporter 1 critically controls microglial activation through facilitating glycolysis. *Molecular Neurodegeneration*, 14(1), 2. <https://doi.org/10.1186/s13024-019-0305-9>
- Wohleb, E. S., Terwilliger, R., Duman, C. H., & Duman, R. S. (2018). Stress-induced neuronal colony stimulating factor 1 provokes microglia-mediated neuronal remodeling and depressive-like behavior. *Biological Psychiatry*, 83(1), 38–49. <https://doi.org/10.1016/j.biopsych.2017.05.026>
- Woodburn, S. C., Bollinger, J. L., & Wohleb, E. S. (2021). The semantics of microglia activation: Neuroinflammation, homeostasis, and stress. *Journal of Neuroinflammation*, 18(1), 258. <https://doi.org/10.1186/s12974-021-02309-6>
- Yan, M., Bo, X., Zhang, J., Liu, S., Li, X., Liao, Y., ... Cheng, J. (2023). Bergapten alleviates depression-like behavior by inhibiting cyclooxygenase 2 activity and NF- κ B/MAPK signaling pathway in microglia. *Experimental Neurology*, 365, Article 114426. <https://doi.org/10.1016/j.expneurol.2023.114426>
- Yin, R., Zhang, K., Li, Y., Tang, Z., Zheng, R., Ma, Y., ... Xie, Y. (2023). Lipopolysaccharide-induced depression-like model in mice: Meta-analysis and systematic evaluation. *Frontiers in Immunology*, 14, 1181973. <https://doi.org/10.3389/fimmu.2023.1181973>
- Yu, X., Yao, H., Zhang, X., Liu, L., Liu, S., & Dong, Y. (2022). Comparison of LPS and MS-induced depressive mouse model: Behavior, inflammation and biochemical changes. *BMC Psychiatry*, 22(1), 590. <https://doi.org/10.1186/s12888-022-04233-2>
- Zhang, L., Zhang, J., & You, Z. (2018). Switching of the microglial activation phenotype is a possible treatment for depression disorder. *Frontiers in Cellular Neuroscience*, 12, 306. <https://doi.org/10.3389/fncel.2018.00306>
- Zhang, X., He, T., Wu, Z., Wang, Y., Liu, H., Zhang, B., ... Yang, C. (2024). The role of CD38 in inflammation-induced depression-like behavior and the antidepressant effect of (R)-ketamine. *Brain, Behavior, and Immunity*, 115, 64–79. <https://doi.org/10.1016/j.bbi.2023.09.026>
- Zhong, L., Sheng, X., Wang, W., Li, Y., Zhuo, R., Wang, K., ... Chen, X. F. (2023). TREM2 receptor protects against complement-mediated synaptic loss by binding to complement C1q during neurodegeneration. *Immunity*, 56(8), 1794–1808 e1798. <https://doi.org/10.1016/j.immuni.2023.06.016>